THE 4TH INTERNATIONAL CONFERENCE ON ALUMINUM ALLOYS

# ELEVATED TEMPERATURE PROPERTIES OF ALUMINUM LITHIUM ALLOYS

J. Albrecht and G. Lütjering
Technical University Hamburg-Harburg, 21071 Hamburg, Germany

## Abstract

The properties of the Al-Li alloy 8090 were investigated in the temperature range of 20°C to 150°C. Emphasis was on the tensile, fatigue (HCF), and creep properties. Two different aging treatments were applied: a two-step treatment incorporating a first aging at a relatively high temperature, followed by a second step at lower temperature, and a conventional single-step aging treatment. The properties of 8090 are compared with those of the conventional high temperature Al-alloy 2618. Comparisons are also made with a previously investigated P/M Al-Li alloy.

## Introduction

Among the group of high strength Al-alloys, Al-Li alloys receive particular interest for aerospace applications due to their unique combination of reduced density and increased stiffness, offering a great potential for weight savings.

Various aluminum-lithium alloys were developed commercially, both conventionally processed (ingot-metallurgy, I/M) like alloy 8090, and powder metallurgy (P/M) processed from rapidly solidified material, like Allied-Signal's alloy 644 B.

The main interest in these alloys is for room temperature or cryogenic temperature applications. Due to the specific properties and structure of the major strengthening δ'-phase, it can be assumed that these alloys have a potential for applications at moderately elevated temperatures (up to 150°C). The δ'-phase is the ordered intermetallic $Al_3Li$-phase, which is coherent with the Al-matrix over a fairly large size range, offering an extended "window" for aging treatments.

Several authors have reported on elevated temperature properties of I/M Al-Li alloys (1-3) and of the P/M-alloy 644 B (4); the properties of a P/M-alloy of similar composition at higher temperature were reported previously (5,6) and will be to some extent included in this paper for comparison.

The current investigations are a consecution of these investigations (5,6) and are focussed on the microstructure and properties of the I/M Al-Li alloy 8090. Tensile, fatigue (HCF) and creep properties were measured at temperatures up to 150°C. Besides a conventional, single-step aging treatment, a modified, two-step treatment was applied, consisting of a first aging step at fairly high temperature and a second step at a lower temperature relatively close to the maximum service temperature. The purpose was to investigate the influence of the aging treatments on thermal stability.

For comparison, the properties of the well known conventional elevated temperature Al-alloy 2618 were investigated in the same temperature range. Some properties of the previously investigated P/M Al-Li alloy (5,6) will be included in the discussion.

## Experimental

The chemical composition of 8090 and 2618 is shown in Table I; for comparison, the composition of the P/M Al-Li alloy is included. The test material of alloy 8090 was supplied by Otto Fuchs Metallwerke, Meinerzhagen, in form of a die forging, solution treated, water quenched and subsequently 3 % cold upset. Specimen blanks, cut with the load axis parallel to the main flow direction of the forging, were subjected to two different aging treatments: a single-step treatment of 27 h at 170°C, and a two-step treatment, consisting of a first step at 210°C for 5 hours, followed by a second step at 170°C for 24 hours.

The alloy 2618 was also supplied by Otto Fuchs Metallwerke in the form of a die forging in the fully heat treated condition (T6). To obtain information about the thermal stability, specimens of both alloys were subjected to an additional heat treatment at 150°C for 500 hours. Tensile tests were performed at 20°C and 150°C, both in the as-aged condition as well as after the 500 h exposure. HCF-tests were also done at 150°C for both alloys and at 20°C for 8090; the room temperature S-N-curve for 2618 was taken from the literature (7). The tests were done at an R-ratio of - 1 at a frequency of about 95 Hz using hour-glass shaped specimens with electrolytically polished surfaces. Creep tests were performed at 150°C; the plastic strain after a test period of 100 hours at a given stress level was used as a measure of creep resistance.

## Results and Discussion

### Microstructure

The grain structure of 8090 and 2618 is shown in Fig. 1. Fig. 1a shows a light-micrograph of alloy 8090 with the typical pancake grain structure. The grains are elongated in the flow direction of the forging up to 200 µm, the thickness of the "pancakes" in the short transverse direction is about 20 µm. At higher magnifications a fine subgrain structure with a cell size of 10 - 20 µm becomes visible. The pancake grain structure of alloy 2618 (Fig. 1b) is not as pronounced as in 8090; the length of the grains is about 200 µm, the thickness about 100 µm. The subgrain structure with a cell size of 20 - 30 µm is clearly visible in Fig. 1b. Alloy 2618 contains a large amount of coarse (several µm) particles, preferentially located in grain boundaries.

The precipitate structure of the alloys, imaged by transmission electron microscopy, is shown in Fig. 2. At lower magnification, alloy 8090 shows after two-step aging discontinuously precipitated S'-phase (Fig. 2a), nucleated at dislocations stemming from the cold deformation after quenching. The higher mangfication darkfield micrograph of 8090 (Fig. 2b) shows precipitates of $Al_3Li$ ($\delta'$), of which two types are observed: "solid" $\delta'$-precipitates with a size of up to 200 Å, and occasional composite precipitates, consisting of a nucleus of fine dispersoids of $Al_3Zr$ with a shell of $\delta'$, having a total diameter of 500-600 Å. These composite precipitates appear ringlike in the darkfield micrograph. In comparison, after single-step aging the precipitates were found to be quite similar with slightly smaller $\delta'$-precipitates and hardly any difference in the S'-population. In addition, narrow precipitate free zones along high-angle grain boundaries were observed in both aging conditions with small particles ($< 0.1$ µm) of the equilibrium $\delta$-phase (AlLi) in the grain boundaries. The amount of intergranular $\delta$-phase was slightly higher after two-step aging. TEM micrographs of alloy 2618 are shown in Fig. 2c and Fig. 2d. The alloy is strengthened by precipitates of S' (Fig. 2a), which are fairly homogeneously distributed except for some areas, where coarse S-phase particles are observed as shown in Fig. 2c. A large difference between the two alloys is found for the grain boundaries: the boundaries in alloy 2618 are densely, sometimes nearly continuously, covered with particles (Fig. 2d) of the type $Al_9FeNi$.

### Tensile Properties

The tensile properties of the two alloys are shown in Table II, in addition, the yield stress and the ductility are shown in Figs. 3a and 3b. The table and the figures also include the tensile properties after the pre-exposure treatment of 500 h at 150°C.

At room temperature, the highest yield stress for unexposed material is found for 8090 after two-step aging (435 MPa), while the yield stress after single-step aging is 375 MPa. Hardness tests verified, that the single-step aging treatment applied here (27 h at 170°C) leads to a slightly underaged condition; the hardness continues to increase slightly up to about 200 hours, while the two-step aging treatment leads to a peak aged condition for the time-temperature combination chosen here. This explains the difference of the room temperature yield stress between these two conditions. It also explains the response of the yield stress to the pre-exposure treatment. The yield stress of the single-step aged material increases after pre-exposure from 375 MPa to 425 MPa, indicative of continued aging, while the yield stress of the two-step aged material decreases by 10 MPa, indicative of a fairly stable precipitate structure after the aging treatment. Alloy 2618 has the lowest yield stress at room temperature (340 MPa in the as-aged condition). An increase of 30 MPa in the yield stress is observed after pre-exposure.

The yield stress values at 150°C show exactly the same tendencies as observed at room temperature: alloy 8090 in the two-step aged condition has the highest yield stress (410 MPa as aged), which remains practically constant after pre-exposure (405 MPa). The single-step aged material has a yield stress of 370 MPa in the as-aged condition, which increases to 405 MPa after pre-exposure. As at room temperature, this finding is indicative of inferior thermal stability of the single-step aged condition as compared to the two-step aged condition. The yield stress of alloy 2618 at 150°C is 325 MPa, increasing to 365 MPa after pre-exposure.

The ductility (true fracture strain $\varepsilon_F = \ln A_o/A$) at room temperature and 150°C is shown in Fig. 3b and Table II. The highest ductility at room temperature is found for 8090 after two-step aging ($\varepsilon_F = 0.22$), while the ductility of the same alloy after single-step aging is only slightly lower ($\varepsilon_F = 0.20$). The lowest ductility is found for 2618 ($\varepsilon_F = 0.15$). The lower ductility of this alloy can be explained by the higher volume fraction of brittle intermetallic phases at grain boundaries. Fractographic examinations of the fracture surfaces showed intergranular fracture for 8090 in both heat treatment conditions, and intergranular fracture with small contributions of ductile, dimpled fracture for 2618.

The pre-exposure treatment decreased the ductility of 8090 in the two-step aged condition considerably from 0.22 to 0.08, while an increase was observed for the same alloy in the single-step aged condition (from 0.20 to 0.27). The fractographic examination showed a considerable amount of intergranular secondary cracking for the two-step aged 8090 material after pre-exposure explaining the decrease of ductility, while no significant changes in fracture mode were observed for the single-step aged material. For alloy 2618, the ductility decreases slightly from 0.15 to 0.12 after pre-exposure, simultaneously, the amount of ductile, dimpled fracture decreases.

At a test temperature of 150°C, the same ranking of the ductilities of the unexposed material is observed: the highest value for alloy 8090 with two-step aging (0.51), closely followed by the single-step aged condition (0.46), and the lowest value for 2618 (0.32).

The pre-exposure treatment has little effect on the ductility of 8090 in both aging conditions, while alloy 2618 shows a strong response: the ductility decreases from 0.32 to 0.12 at 150°C.

Fatigue Properties

The fatigue properties of alloy 8090 for both aging conditions was tested at RT and 150°C, the S-N curve of 2618 at 150°C. For comparison, literature data (7) for the RT-fatigue curve of 2618 are included.

At room temperature (Fig. 4a), the fatigue strength of all three conditions is quite similar: 140 MPa for 8090 in the two-step aged condition and for 2618, and a slightly higher value of 160 MPa for 8090 after single-step aging. The difference in fatigue strength between 8090 and 2618 is more pronounced at a test temperature of 150°C (Fig. 4b); here the fatigue strength of

both 8090-conditions (about 130 MPa) remains close to the room temperature values (140 or 160 MPa, resp.), while the fatigue strength of 2618 decreases considerably to about 90 MPa.

Creep Properties

The creep properties of the three conditions were measured at a temperature of 150°C; in this investigation, a load of 225 MPa was applied. The plastic strain after a test period of 100 hours was used as a measure of the creep resistance. As shown in Table III, the creep behavior of alloy 8090 in both aging conditions is the same: 0.15 % plastic strain after 100 hours, while the creep strain of 2618 is considerably lower (0.08 %).

For comparison, results of the previous investigation (5,6) are included here, where 8090 (two-step aging), and 2618, and in addition the P/M-alloy Al-2.1Li-1.2Cu-0.6Mg-0.7Ti-0.7Zr-1Mn (two-step aging) were tested at different stress levels, as shown in Fig. 5. By far the highest creep strains were found for the P/M-alloy; at a stress of 225 MPa, for example, the P/M-alloy has a creep strain of 1.2 %, compared to 0.15 % for 8090 and 0.08 % for 2618.

This behavior is indicative of grain boundary sliding as the controlling mechanism for creep deformation. The grain size of the P/M alloy is extremely small ($\approx 1\mu m$) compared to the conventional alloys; furthermore, there are only very fine and small particles in the grain boundaries to hinder sliding. Comparing alloys 8090 and 2618, the latter contains a much higher amount of grain boundary particles (c.f. Figs. 2a and 2d), explaining the lower creep strain of 2618. Assuming that grain size and amount of grain boundary particles are dominating parameters for creep deformation, it is obvious that no noticeable difference in the creep behavior of the two conditions of 8090 (two-step and single-step aging) were observed.

Conclusions

The aluminum-lithium alloy 8090 shows attractive elevated temperature properties up to 150°C in comparison with the conventional elevated temperature Al-alloy 2618.

Emphasis in this investigation was on the influence of the aging treatment on the properties, particularly at elevated temperatures. A conventional, single step aging treatment (27h at 170°C) was compared with a two-step aging treatment (5h at 210°C + 24h at 170°C); the two step aging treatment resulted in a better thermal stability, as verified by tensile tests after a pre-exposure of 500h at 150°C. In comparison with alloy 2618, the two-step aged alloy 8090 shows:

- Higher yield stress at room temperature (+ 40 MPa) and at 150°C (+ 50 MPa).
- Higher ductility over the whole temperature range.
- Better fatigue strength, particularly at 150°C (+ 30 MPa).
- Slightly inferior creep resistance at 150°C, due to the lower content of particles in the grain boundaries.
- The thermal stability of 8090 after two-step aging is comparable to that of 2618.

A lithium containing, P/M-processed alloy exhibits much higher yield stress and superior fatigue strength as compared to alloy 8090, however, the creep resistance is quite poor due to the small grain size, which makes the P/M-alloy unfavourable for creep-controlled applications. It is anticipated, that the elevated temperature properties, including the creep resistance, of the alloy 8090 can be further improved by optimizing the two-step aging treatment.

Acknowledgement

This work received support by the "Stifterverband Metalle", Düsseldorf, Germany. The authors wish to thank Dr. Fischer, Otto Fuchs Metallwerke, Meinerzhagen, for supplying the test materials.

## References


1. M. Pridham, B. Noble, S.J. Harris: Elevated Temperature Strength of Al-Li-Cu-Mg-Alloys, in: Al-Li-Alloys III, eds.: C. Baker, P.J. Gregson, S.J. Harris, C.J. Peel; Proc. 3rd Intern. Al-Li Conference, The Institute of Metals, London, 1986, p.547.

2. X. Xiaoxiu, J.W. Martin: J. Mat. Sci. 27 (1992), p.592.

3. C.K.L. Davies et al., J. Mat. Sci. 27 (1992), p.3953.

4. J.C. LaSalle: Elevated Temperature Properties of an RS/PM Aluminium-Lithium Alloy, in: Proc. of the "P/M in Aerospace and Defense Technology" Symp., eds.: F.H. Froes, Princeton, N.J., USA, 1991, p.373.

5. U.K. Habel, Ph.D. thesis, Techn. Univ. Hamburg-Harburg, Hamburg, Germany (1993).

6. J. Albrecht et al., Structure and Properties of P/M-Aluminum Alloys, in "Light Weight Alloys for Aerospace Applications II", eds.: E.W. Lee, N.J. Kim, TMS (1991), p.77.

7. Aerospace Structural Metals Handbook, Dept. of Defense; Belfour Stulen, Inc., USA (1975).


Table I: Chemical composition of 8090 and 2618, P/M-Al-Li alloy (5,6) for comparison

| Alloy | Li | Cu | Mg | Zr | Ti | Mn | Fe | Ni | Al |
|---|---|---|---|---|---|---|---|---|---|
| 8090 | 2.4 | 1.2 | 0.9 | 0.1 | -- | -- | -- | -- | Bal. |
| 2618 | -- | 2.5 | 1.5 | -- | 0.1 | -- | 1.0 | 1.2 | Bal. |
| P/M Al-Li | 2.1 | 1.2 | 0.6 | 0.7 | 0.7 | 1.0 | -- | -- | Bal. |

Table II. Tensile properties at 20°C and 150°C with (500) and without (0) pre-exposure

| Condition | Pre-Exposure | Test temp.(°C) | $\sigma_{0.2}$ (MPa) | UTS (MPa) | $\sigma_F$ (MPa) | El. (%) | $\varepsilon_F$ |
|---|---|---|---|---|---|---|---|
| 8090 single-step | 0 | 20°C | 375 | 495 | 595 | 10.6 | 0.20 |
| | 500h | 20°C | 425 | 525 | 640 | 8.7 | 0.27 |
| 8090 two-step | 0 | 20°C | 435 | 515 | 645 | 11.0 | 0.22 |
| | 500h | 20°C | 422 | 510 | 560 | 8.0 | 0.08 |
| 2618 | 0 | 20°C | 340 | 425 | 490 | 8.0 | 0.15 |
| | 500h | 20°C | 370 | 435 | 490 | 7.3 | 0.12 |
| 8090 single-step | 0 | 150°C | 370 | 430 | 590 | 14.1 | 0.46 |
| | 500h | 150°C | 405 | 425 | 560 | 16.9 | 0.53 |
| 8090 two-step | 0 | 150°C | 410 | 435 | 560 | 18.0 | 0.51 |
| | 500h | 150°C | 405 | 425 | 545 | 17.8 | 0.49 |
| 2618 | 0 | 150°C | 325 | 380 | 480 | 12.8 | 0.32 |
| | 500h | 150°C | 365 | 390 | 425 | 7.6 | 0.12 |

Table III. Creep strain at 225 MPa and 150°C after 100 hours

| Alloy | $\varepsilon_{pl,100h}$ (%) |
|---|---|
| 8090 single-step | 0.15 |
| 8090 two-step | 0.15 |
| 2618 | 0.08 |

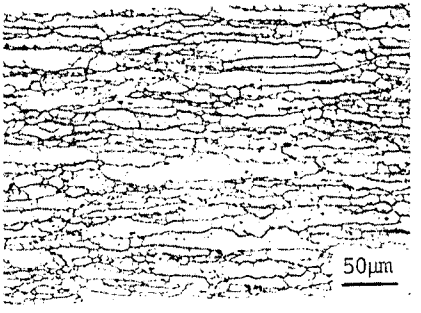


a) 8090

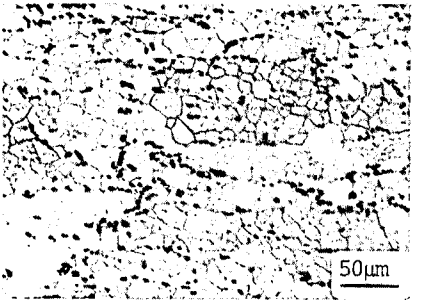


b) 2618

Fig. 1: Grain structure of the two alloys (LM)

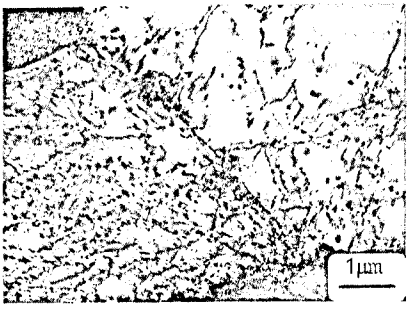


a) 8090 (S' and GB precipitates)

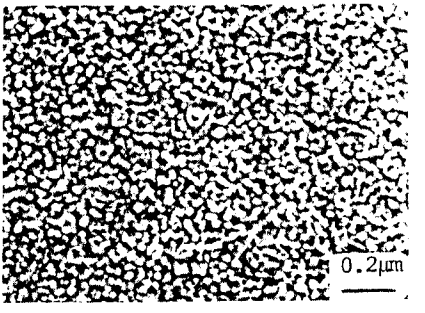


d) 8090 (δ'-precipitates)


c) 2618 (S' and S precip.)

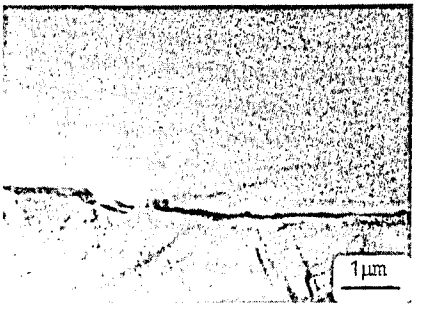


d) 2618 (GB particles)

Fig. 2: Microstructure of the two alloys (TEM); 8090 in the two-step aged condition

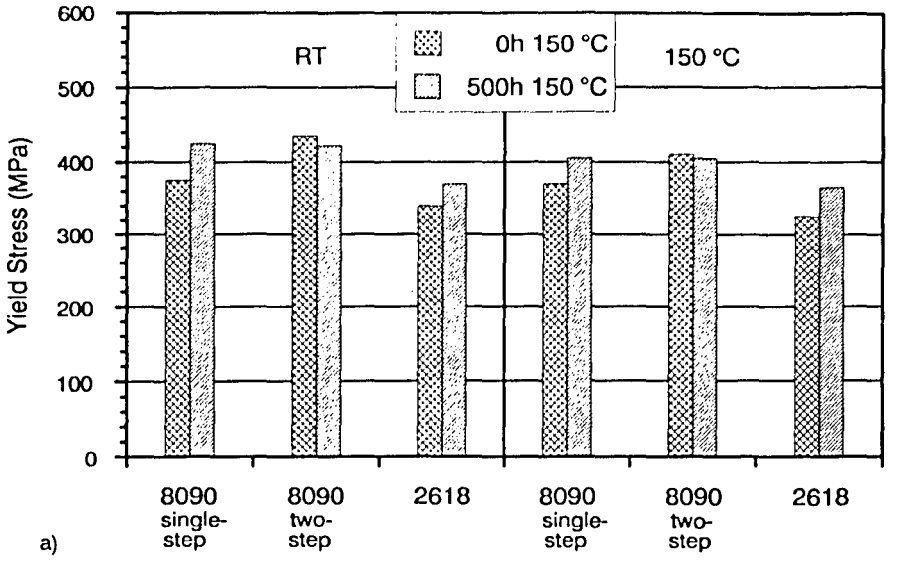


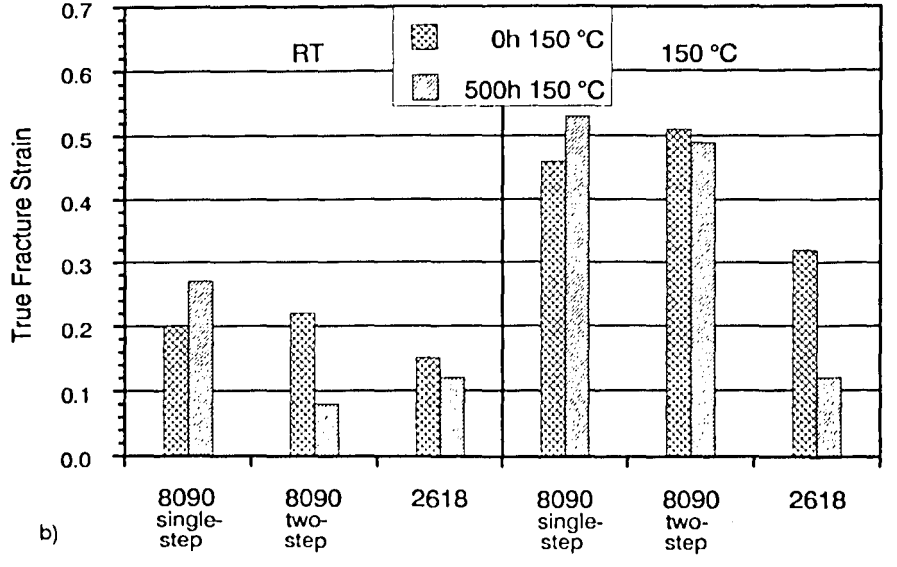


Fig. 3: Tensile properties at RT and 150°C without and with pre-exposure
a) Yield stress
b) Ductility

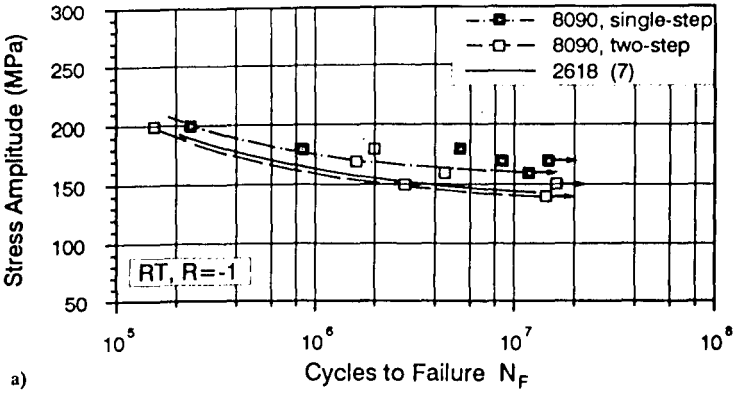


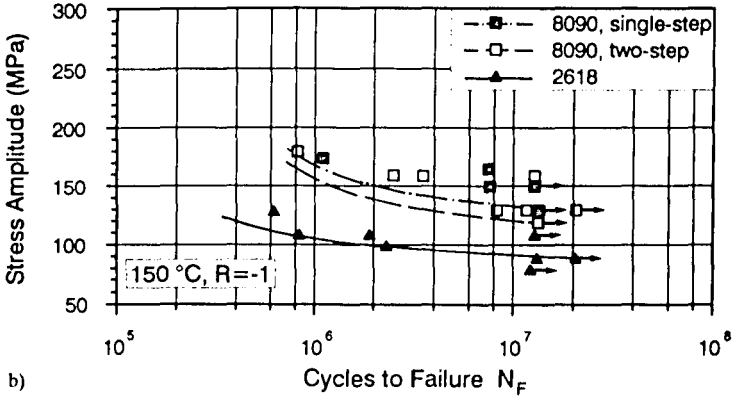


Fig. 4: Fatigue properties at RT (a) and 150°C (b)

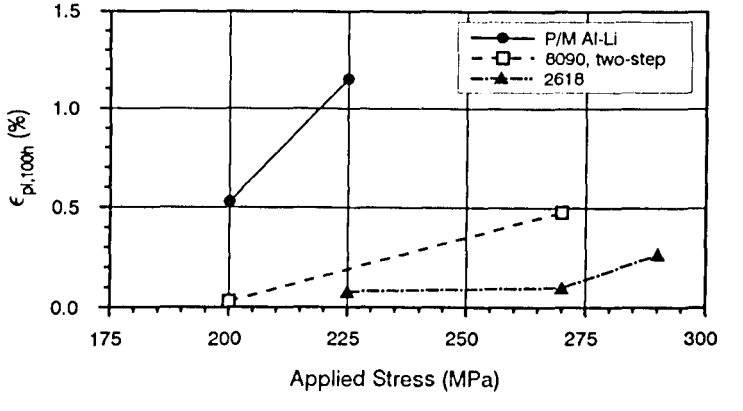


Fig. 5: Creep properties at 150°C of 8090 (two-step aging) and 2618, P/M Al-Li (two-step aging) for comparison